Stochastic Planning of a Campus Microgrid Considering Practical CHP and Market Constraints

Masoud Hajian Foroushani
Electrical and Software Engineering Department
University of Calgary
Calgary, Canada
masoud.hajianforoush@ucalgary.ca

Mostafa Farrokhabadi
Electrical and Software Engineering Department
University of Calgary
Calgary, Canada
mostafa.farrokhabadi@ucalgary.ca

***Abstract*—This paper presents a stochastic planning framework to determine the optimal sizing of BESS and PV for campus microgrids based on realistic data obtained from the University of Calgary campus microgrid. This grid-connected microgrid includes a combined heat and power (CHP) plant and a 400 kW solar photovoltaic (PV) system. Driven by campus mandates for efficiency, reliability, and sustainability, the planning framework studies and identifies the optimal investment scenario for upgrading the existing PV capacity and incorporating a battery energy storage system (BESS). The practical framework integrates the operational intricacies of the CHP plant and the modeling complexities of the Alberta electricity market, including the pool price and the nonlinear transmission and distribution fees (T&D). By considering various stochastic scenarios regarding electricity price, load growth, and gas price, the study develops a daily optimization approach to consider the intricacies of the electricity market, formulating the optimization framework as a mixed-integer linear programming stochastic problem. Reported key performance metrics include the net present cost (NPC) and the saving-to-investment ratio (SIR) over the planning horizon. Results support investing in distributed energy resources (DERs) to reduce the supplied cost of energy.**

***Index Terms*—Microgrid, Planning, Optimization, CHP, DERs.**

I Introduction

Driven by sustainability, economic efficiency, and resiliency mandates, university campuses worldwide are considering shifting toward a more localized and sustainable approach to supplying their electrical demand [1]. In this context, microgrids have been the focus of research to meet the operational requirements of contemporary campuses worldwide. Microgrids are formally defined as a group of interconnected loads and distributed energy resources (DERs) that act as a single controllable entity and can operate in the grid-connected or islanded modes of operation [2].

Limited works have discussed the planning and operation of university campus microgrids. For example, [3] discusses the optimization of the thermal and electrical demand of the University of California, San Diego, aimed at minimizing the operating cost and providing ancillary services. Moreover, [4] proposes an energy management system (EMS) for the University of Engineering and Technology (UET) campus that includes a battery energy storage system (BESS), solar photovoltaics (PV), and microturbines. The proposed EMS considers the uncertainties in solar irradiance and electricity demand. Moreover, the authors in [5], investigate the planning and operation of the University of Guelph campus microgrid, where the incorporation of a combined heat and power (CHP) plant with different fuel types is studied, considering the investment cost, fuel cost, operation and maintenance cost, electricity cost, and profits made by selling electricity. Similarly, [6] performs a techno-economic analysis of BESS and PV planning and operation for a campus microgrid in Seoul, South Korea. The paper considers various incentive programs, such as energy arbitrage and peak shaving, maximizing discounted revenues over a planning horizon of 25 years. This study assumes a deterministic case study where the impact of uncertainties associated with the random variables is not handled.

A considerable body of prior art has investigated the planning and optimal operation of microgrids. For instance, [7] discusses the optimal operation of multiple CHP plants within an AC microgrid with the objective of reducing the costs, and [8] analyzes the optimal operation of hybrid microgrids in the presence of renewable and distributed energy resources. In addition to cost minimization, reducing emissions and environmental costs have also been discussed in the research papers. For example, [9] formulates a day-ahead optimal dispatch to reduce environmental and operation costs in a microgrid containing CHP plants and renewable energy resources (RES). Similarly, [10] proposes a sustainable EMS that incorporates DERs emissions and demand response in a microgrid. The microgrid consists of PV, wind, and CO2-emitting DERs. Moreover, the authors in [11] propose a two-part deterministic EMS for a microgrid; the central EMS provides the forecast for PV and load as well as setpoints for dispatchable units, and the local power management handles voltage and frequency regulation. Furthermore, [12] presents a physics-informed neural network to lower the operating cost of a microgrid. The physics-informed approach is implemented using a convolutional neural network (CNN) with the constraints incorporated into the loss function. The proposed CNN-based framework achieves accurate results while accelerating optimization runtime by 400 times in a deterministic study. The authors in [13] discuss the incorporation of large-scale electric vehicles to lower the operation and environmental costs. Some research has also considered the impact of thermal demand in

the microgrid EMS. For example, [14] and [15] investigate the minimum cost of microgrid operation while considering the thermal demand constraints.

On the planning side, [16] proposes a two-stage framework, in which the optimal size of different components is determined in the first stage, and the operating cost of the microgrid is minimized in the second stage. In addition, [17] presents a bi-level approach, in which the upper-level deals with the optimal sizing of the electrolyzer and hydrogen storage, while the lower level optimizes their operation. Furthermore, [18] explores the planning for a microgrid considering the lifetime of the energy storage system, including factors such as complete/incomplete cycles and thermal impacts. In addition, [19] considers the planning for a residential microgrid consisting of PV and a hybrid of BESS and thermal energy storage systems. This paper also presents a comprehensive sensitivity analysis of the electricity price, storage size, and PV capacity on the payback period, demonstrating that higher electricity prices favor the payback period.

In view of the abovementioned works, and considering the relative scarcity of planning studies of a real-world campus microgrid, this paper presents a 15-year stochastic planning framework for the University of Calgary campus microgrid [1], located in Calgary, Alberta, Canada. The microgrid is connected to the distribution network via multiple points of interconnection and includes a CHP plant and on-campus PV. Thus, the planning framework calculates the operation costs of a set of pre-defined BESS and PV sizes, considering the uncertainties regarding the electricity price and demand as well as the gas price. In addition, without losing the generality, the framework considers, for the first time in similar studies, the practical nuances of the electricity market in Alberta, Canada. Similar market characteristics can be found in other jurisdictions such as Ontario, California, etc. Thus, the contributions of this paper are as follows:

- Utilizing actual operation data from the University of Calgary campus microgrid and the electricity price from the Alberta Electric System Operator (AESO).
- Modeling the Alberta electricity market in detail, where the electricity pool price is set by AESO and Transmission and Distribution (T&D) fees are collected by the distribution facility owners (DFOs).
- Developing a stochastic 15-year planning for the University of Calgary campus microgrid, considering the BESS lifetime, realistic plant constraints, and practical campus operation needs.

The rest of the paper is organized as follows: Section II details the optimization model. Section III presents the test system, data, scenarios, and numerical results. Finally, Section IV provides conclusions and future work.

II Optimization Framework

The proposed mixed-integer linear programming framework iterates over a set of pre-defined PV and BESS sizes and optimizes the operation costs over a certain planning horizon. The optimization is performed on a daily basis; to reduce the computational burden, the optimization considers every 5$^{\text{th}}$ day of operation. Thus, the scaling parameter $\gamma = 5$ is used to adjust for the planning period. The objective function and constraints are presented in the following subsections.

A. Objective Function

The objective function comprises capital costs for the BESS and additional PV units and the discounted value of campus operation costs, including CHP plant generation costs, operation and maintenance (O&M) costs for PV and BESS, cost of purchasing power from the grid, and the revenue earned by selling power back to the grid. The mathematical formulation for the objective function, $\mathcal{O}$, is as follows:

$$\mathcal{O} = \sum_{\omega \in \Omega} P_{\omega} \times \left[C^{\text{inv}} + \sum_{y \in \mathcal{Y}} \sum_{d \in \mathcal{D}} \frac{C^{\text{op}}_{\omega,y,d}}{(1+r)^{y-1}} \right] \tag{1}$$

where Ω, $\mathcal{Y}$, and $\mathcal{D}$ are the sets for scenarios, years, and days, respectively. P_{ω} represents the probability of each scenario ω, C^{inv} is the investment cost, r is the discount rate, and $C^{\text{op}}_{\omega,y,d}$ represents the operation cost of the campus for scenario ω, year y, and day d. The investment cost C^{inv} and the operation cost $C^{\text{op}}_{\omega,y,d}$ are defined as follows:

$$C^{\text{inv}} = K^{\text{pv}} \times (I^{\text{pv}} - I^{\text{pv}}_{\text{existing}}) + K^{\text{BESS}} \times I^{\text{BESS}} \tag{2}$$

$$C^{\text{op}}_{\omega,y,d} = C^{\text{CHP}}_{\omega,y,d} + C^{\text{O\&M}}_{\omega,y,d} + C^{\text{b}}_{\omega,y,d} - C^{\text{s}}_{\omega,y,d} \tag{3}$$

where K^{pv} and K^{BESS} are the investment costs of PV and BESS in \$/MW , respectively. Additionally, I^{pv} and I^{BESS} represent the installed capacities of the PV and BESS systems, while $I^{\text{pv}}_{\text{existing}}$ denotes the existing PV capacity. Moreover, the operation cost of the campus comprises four components: the cost of electricity generated by the CHP plant, $C^{\text{CHP}}_{\omega,y,d}$, the O&M cost for PV and BESS, $C^{\text{O\&M}}_{\omega,y,d}$, the cost of purchasing electricity from the grid, $C^{\text{b}}_{\omega,y,d}$, and the revenue earned from selling electricity back to the grid, $C^{\text{s}}_{\omega,y,d}$. These components are expressed as follows:

$$C^{\text{CHP}}_{\omega,y,d} = \gamma \times \left[\sum_{h \in \mathcal{H}} P^{\text{CHP}}_{\omega,y,d,h} \times H_{\omega,y,d,h} \right] \tag{4}$$

$$C^{\text{O\&M}}_{\omega,y,d} = \gamma \times \left[c^{\text{pv}} \times \sum_{h \in \mathcal{H}} P^{\text{pv}}_{\omega,y,d,h} + c^{\text{BESS}} \times I^{\text{BESS}} \right] \tag{5}$$

$$C^{\text{s}}_{\omega,y,d} = \gamma \times \left[\sum_{h \in \mathcal{H}} P^{\text{s}}_{\omega,y,d,h} \times \alpha_{\text{pp},\omega,y,d,h} \right] \tag{6}$$

$$C^{\text{b}}_{\omega,y,d} = \gamma \times \left[\sum_{h \in \mathcal{H}} C'^{\text{b}}_{\omega,y,d,h} + C''^{\text{b}}_{\omega,y,d} \right] \tag{7}$$

where $\mathcal{H}$ denotes the set of hours in a day and $P^{\text{CHP}}_{\omega,y,d,h}$ and $H_{\omega,y,d,h}$ are the power generated and heat rate of plant in

[1]The term microgrid is used loosely here given that the campus cannot smoothly transition between connected and islanded operating modes.

MW and \$/MWh for scenario ω, year y, day d, and hour h, respectively. In equation (5), c^{pv} is the unit O&M cost of PV in \$/MWh and $P^{\text{pv}}_{\omega,y,d,h}$ is the output of PV in MW. In contrast to the O&M cost of PV, BESS O&M cost is fixed throughout the year and is represented by c^{BESS} in \$/MW-year. in equation (6), $P^{\text{s}}_{\omega,y,d,h}$ is the power exported to the grid and $\alpha_{\text{pp},\omega,y,d,h}$ represents the electricity pool price in MW and \$/MWh respectively. Furthermore, in (7), $C'^{\text{b}}_{\omega,y,d,h}$ and $C''^{\text{b}}_{\omega,y,d}$ show the hourly and daily cost of electricity in \$, which will be explored in the subsequent subsection.

B. Alberta Electricity Market Structure

The electricity market in Alberta operates under a hierarchical structure. The hourly electricity pool price is determined in the spot market by AESO. Subsequently, DFOs apply additional T&D fees and local access fees (LAF). As a result, some components of the electricity bill are calculated hourly, while others, such as demand charges, are calculated daily. The overall hourly component is formulated as follows:

$$C'^{\text{b}}_{\omega,y,d} = \sum_{h\in\mathcal{H}} \Big(P^{\text{b}}_{\omega,y,d,h} \times \alpha_{\text{pp},\omega,y,d,h} + P^{\text{b}}_{\omega,y,d,h} \times \alpha_{\text{on}} \times e^{\text{on}}_{\omega,y,d,h} + P^{\text{b}}_{\omega,y,d,h} \times \alpha_{\text{off}} \times e^{\text{off}}_{\omega,y,d,h} + P^{\text{b}}_{\omega,y,d,h} \times \alpha_{\text{laf}} \Big) \quad (8)$$

where α_{on}, α_{off}, and α_{laf} represent the electricity rates for on-peak and off-peak times, and LAF in \$/MWh respectively. Time-of-use (TOU) pricing defines the on-peak period as 8:00 a.m. to 9:00 p.m. on weekdays, excluding weekends and statutory holidays. Other times are considered off-peak. Additionally, $e^{\text{on}}_{\omega,y,d,h}$ and $e^{\text{off}}_{\omega,y,d,h}$ are binary parameters that indicate the TOU status of the hour.

The electricity bill daily component is as follows:

$$C''^{\text{b}}_{\omega,y,d} = \alpha_{\text{sc}} + V_{\omega,y,d} \times \alpha_{\text{nrdc}} + b_{\omega,y,d} \times \alpha_{\text{fc}} + b_{\omega,y,d} \times \alpha_{\text{dc}} \quad (9)$$

where α_{sc} denotes the fixed service charge in \$, and α_{nrdc}, α_{fc}, and α_{dc} represent the rates for the Non-Ratchet Demand Charge, Facility Charge, and Demand Charge, respectively, all in \$/MVA. Furthermore, $b_{\omega,y,d}$ and $V_{\omega,y,d}$ denote the billing demand and the daily peak purchased power in MW. The billing demand is defined as the greater of the daily peak purchased power and 90% of the peak over the previous 365 days, known as the ratchet demand, as follows:

$$b_{\omega,y,d} = \max\left\{ V_{\omega,y,d},\ 0.9 \times \max_{d'\in[d-365,\, d-1]} V_{\omega,y,d'} \right\} \quad (10)$$

The billing demand requires identifying the daily peak power, as shown in (11)–(13). Note that these equations are the linearized form of a maximum function.

$$V_{\omega,y,d} \geq P^{\text{b}}_{\omega,y,d,h} \quad (11)$$

$$V_{\omega,y,d} \leq P^{\text{b}}_{\omega,y,d,h} + (1 - PD_{\omega,y,d,h}) \times M \quad (12)$$

$$\sum_{h\in\mathcal{H}} PD_{\omega,y,d,h} = 1 \quad (13)$$

where $PD_{\omega,y,d,h}$ is a binary variable for peak detection and M is a sufficiently large number. Similarly, $b_{\omega,y,d}$ is linearized by (14)–(17), as follows:

$$b_{\omega,y,d} \geq V_{\omega,y,d} \quad (14)$$

$$b_{\omega,y,d} \geq P^{\text{r}}_{\omega,y,d} \quad (15)$$

$$b_{\omega,y,d} \leq V_{\omega,y,d} + (1 - BD_{\omega,y,d}) \times M \quad (16)$$

$$b_{\omega,y,d} \leq P^{\text{r}}_{\omega,y,d} + BD_{\omega,y,d} \times M \quad (17)$$

where $BD_{\omega,y,d}$ is a binary variable selecting daily peak vs. the ratchet demand, and $P^{\text{r}}_{\omega,y,d}$ is the historical ratchet demand defined in Equation (10).

C. Grid Constraints

To ensure appropriate interactions with the grid, constraint (18) disallows buying and selling power from/to the grid simultaneously, while constraints (19) and (20) impose an upper limit on the power purchased or sold.

$$u^{\text{s}}_{\omega,y,d,h} + u^{\text{b}}_{\omega,y,d,h} \leq 1 \quad (18)$$

$$P^{\text{b}}_{\omega,y,d,h} \leq u^{\text{b}}_{\omega,y,d,h} \times P^{\text{b,max}} \quad (19)$$

$$P^{\text{s}}_{\omega,y,d,h} \leq u^{\text{s}}_{\omega,y,d,h} \times P^{\text{s,max}} \quad (20)$$

where $u^{\text{s}}_{\omega,y,d,h}$ and $u^{\text{b}}_{\omega,y,d,h}$ are binary variables for selling and buying electricity, respectively. Furthermore, $P^{\text{b,max}}$ and $P^{\text{s,max}}$ represent the maximum power limits for buying and selling electricity from/to the grid in MW.

D. CHP Plant Constraints

The CHP plant output is limited by the upper and lower bounds defined in (21) and (22), respectively. Ramp-up and ramp-down limitations are enforced by (23) and (24). Additionally, (25) restricts the number of times the CHP plant can be turned off during its operation. Constraints (26) and (27) ensure that the minimum uptime and downtime requirements of the plant are satisfied.

$$P^{\text{CHP}}_{\omega,y,d,h} \leq P^{\text{CHP,max}} \times u^{\text{on}}_{\omega,y,d,h} \quad (21)$$

$$P^{\text{CHP}}_{\omega,y,d,h} \geq P^{\text{CHP,min}} \times u^{\text{on}}_{\omega,y,d,h} \quad (22)$$

$$P^{\text{CHP}}_{\omega,y,d,h} - P^{\text{CHP}}_{\omega,y,d,h-1} \leq P^{\text{ru}} \quad (23)$$

$$P^{\text{CHP}}_{\omega,y,d,h-1} - P^{\text{CHP}}_{\omega,y,d,h} \leq P^{\text{rd}} \quad (24)$$

$$\sum_{i=1}^{24} 1 - u^{\text{on}}_{\omega,y,d,i} \leq T^{\text{off}} \tag{25}$$

$$\sum_{i=h}^{\min(h+T^{\text{u}}-1,\,|\mathcal{H}|)} u^{\text{on}}_{\omega,y,d,i} \geq (\min(T^{\text{u}},\,|\mathcal{H}|-h+1)) \times \left(u^{\text{on}}_{\omega,y,d,h} - u^{\text{on}}_{\omega,y,d,h-1}\right) \tag{26}$$

$$\sum_{i=h}^{\min(h+T^{\text{d}}-1,\,|\mathcal{H}|)} 1 - u^{\text{on}}_{\omega,y,d,i} \geq \left(\min(T^{\text{d}},\,|\mathcal{H}|-h+1)\right) \times \left(u^{\text{on}}_{\omega,y,d,h-1} - u^{\text{on}}_{\omega,y,d,h}\right) \tag{27}$$

where $P^{\text{CHP,max}}$, $P^{\text{CHP,min}}$, P^{rd} and P^{ru} represent the maximum and minimum CHP plant output power in MW, and the ramp-down and ramp-up limits in MW/h, respectively. Additionally, $|\mathcal{H}|$ denotes the number of hours in a day, while T^{off}, T^{u} and T^{d} are the allowable off-times, minimum uptime, and downtime requirements in hours. Furthermore, $u^{\text{on}}_{\omega,y,d,h}$ is a binary variable which indicates whether the CHP plant is on or off.

E. BESS Constraints

The BESS state-of-charge (SoC) is modeled in (28). In this equation, $\text{SoC}_{\omega,y,d,h}$ represents the SoC of the BESS, E_{tot} is the total energy of the BESS, and η denotes the charging/discharing efficiency. Additionally, $P^{\text{ch}}_{\omega,y,d,h}$ and $P^{\text{dis}}_{\omega,y,d,h}$ show the charging and discharging power of the BESS in MW.

$$\text{SoC}_{\omega,y,d,h} = \text{SoC}_{\omega,y,d,h-1} + \left(\frac{\eta \times P^{\text{ch}}_{\omega,y,d,h}}{E_{\text{tot}}} - \frac{P^{\text{dis}}_{\omega,y,d,h}}{\eta \times E_{\text{tot}}}\right) \tag{28}$$

Constraint (29) prevents simultaneous charging and discharging by utilizing the binary variables $I^{\text{ch}}_{\omega,y,d,h}$ and $I^{\text{dis}}_{\omega,y,d,h}$, which indicate whether the BESS is in charging or discharging mode, respectively. To limit the charging and discharging power of the BESS, constraints (30) and (31) put an upper bound on the charging and discharging power of the BESS. In this regard, $P^{\text{ch,max}}$ and $P^{\text{dis,max}}$ indicate the maximum charging or discharging power respectively.

$$I^{\text{ch}}_{\omega,y,d,h} + I^{\text{dis}}_{\omega,y,d,h} \leq 1 \tag{29}$$

$$P^{\text{ch}}_{\omega,y,d,h} \leq I^{\text{ch}}_{\omega,y,d,h} \times P^{\text{ch,max}} \tag{30}$$

$$P^{\text{dis}}_{\omega,y,d,h} \leq I^{\text{dis}}_{\omega,y,d,h} \times P^{\text{dis,max}} \tag{31}$$

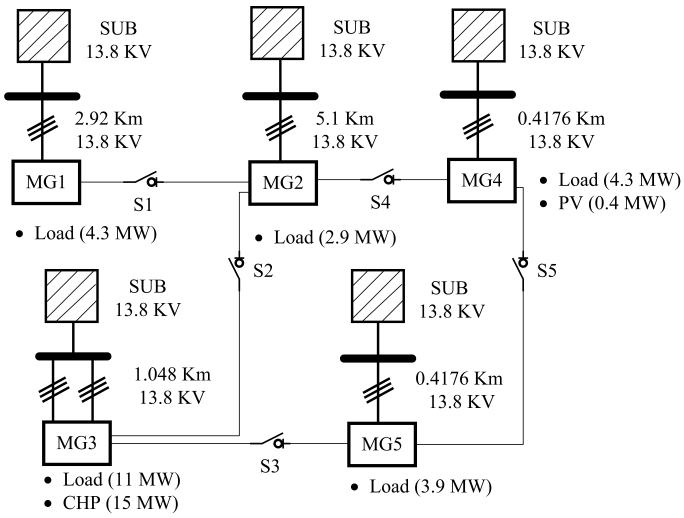

Fig. 1. University of Calgary campus microgrid schematics.

F. Supply-Demand Balance

Constraint (32) ensures that, at any given time, the total supply power is equal to the total demand power, where $P^{\text{d}}_{\omega,y,d,h}$ is the campus electricity demand.

$$P^{\text{d}}_{\omega,y,d,h} + P^{\text{s}}_{\omega,y,d,h} + P^{\text{ch}}_{\omega,y,d,h} = P^{\text{pv}}_{\omega,y,d,h} + P^{\text{CHP}}_{\omega,y,d,h} + P^{\text{dis}}_{\omega,y,d,h} + P^{\text{b}}_{\omega,y,d,h} \tag{32}$$

III Optimization Results

A. Test System

The test system is based on the University of Calgary campus microgrid, as shown in Fig. 1. The system is made up of 5 islands, which are disconnected in the default operating mode. The Islands are supplied by three different distribution substations. For simplicity, this study assumes that all microgrids are unified and that the campus exchanges energy with the upstream grid as a single entity. We defer the electrical consideration of this networked microgrid structure to future works, as explained in Section IV.

B. Data

The presented study is based on realistic data from the campus microgrid and the Alberta electricity market. The optimization scenarios are based on the data for 2023. The annual load and PV generation profiles are depicted in Figures 2 and 3. Figure 4 illustrates the electricity pool price [20]. Other components of the electricity bill, such as T&D fees are presented in Table I. The LAF rate is 15.507 $/MWh [21]. The big M values for linearizing max functions are 5 and 2.79 for the base case and cases with BESS and additional PV.

The real discount rate is assumed 2.75%, and the nominal discount rate is calculated using the Fisher equation and considering Canada's inflation rate, which is equal to 2.6%. Moreover, the BESS and PV capital costs are presented in Table II [22], [23]. A contribution of this paper is the realistic

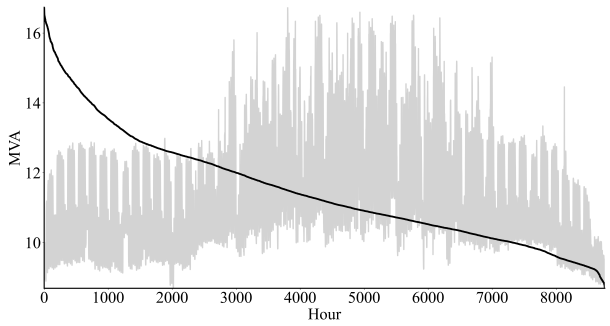

Fig. 2. Campus load profile and its duration curve.

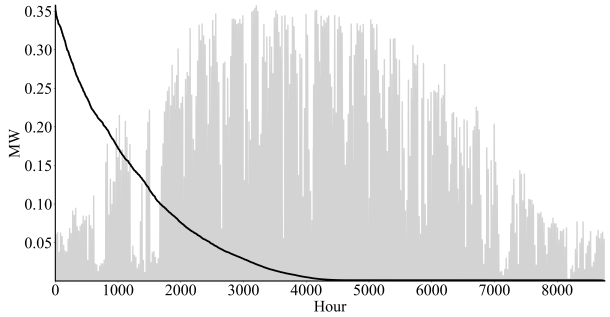

Fig. 3. PV generation profile and its duration curve.

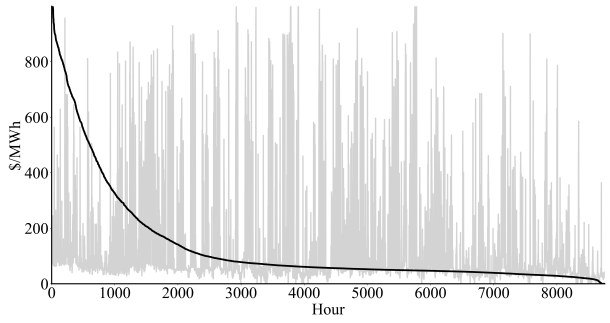

Fig. 4. Alberta electricity pool price and its duration curve.

modeling of the CHP plant heat rate and maximum output functions according to the turbine manufacturer specification [24]. Thus, a temperature-dependent CHP plant heat rate and maximum power output are estimated by fitting quadratic regression models to operation data obtained from turbine characteristic curves. The results are shown in Figure 5, achieving mean absolute percentage errors (MAPE) of 0.24% and 0.35%, respectively. The historical ambient temperature, used for the regression, is illustrated in Fig. 6. Table III summarizes key operational values of the CHP plant provided by the University Facilities Team. The minimum output of the CHP plant is set to 50% of the theoretical maximum output, $P_{\text{th}}^{\text{CHP,max}}$, which is dictated by the maximum output power curve in Figure 5. Furthermore, the maximum output of the CHP plant is set as the minimum of $P_{\text{th}}^{\text{CHP,max}}$ and $P_{\text{pr}}^{\text{CHP,max}}$, which is the practical CHP plant output.

TABLE I
TRANSMISSION AND DISTRIBUTION FEE PARAMETERS [25]

Parameter	Value	Parameter	Value
α_{sc}	29.879	α_{dc}	298.788
α_{fc}	20.845	α_{on}	9.979
α_{nrdc}	60.092	α_{off}	7.325

TABLE II
BESS AND PV PARAMETERS

Parameter	Value	Parameter	Value
K^{BESS}	2917.83×10^3	$P^{\text{ch,max}}$, $P^{\text{dis,max}}$	$\{0.5,\ 1,\ 2\}$
c^{BESS}	70.31×10^3	K^{pv}	1245.53×10^3
η	0.92	c^{pv}	0.0035×10^3
BESS Lifetime	15 years	PV Lifetime	20 years

TABLE III
CHP PLANT OPERATION PARAMETERS

Parameter	Value	Parameter	Value
P^{rd}	10	P^{ru}	10
$P^{\text{b,max}}$	10	$P^{\text{s,max}}$	10
$P_{\text{pr}}^{\text{CHP,max}}$	15	$P^{\text{CHP,min}}$	$0.5 \times P_{\text{th}}^{\text{CHP,max}}$
T^{u}	5	T^{d}	5
T^{off}	6		

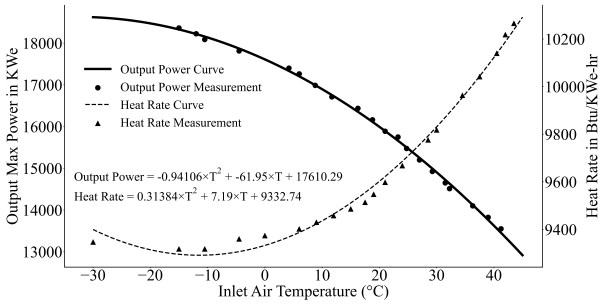

Fig. 5. CHP plant turbine characteristics.

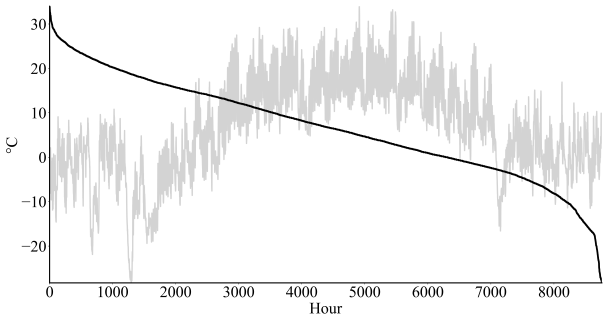

Fig. 6. Ambient temperature and its duration curve.

C. Scenarios

To account for uncertainties in electricity and gas prices as well as load, this study generates multiple growth scenarios. For the gas price, forecasted values from [26] are used to generate a base and a high-growth profile. A 1% and 5%

TABLE IV
OPERATIONAL COST, TOTAL COST, INVESTMENT SUMMARY, SAVINGS, AND SIR FOR DIFFERENT PV AND BESS CONFIGURATIONS

BESS Cap	PV Cap	Operational NPC ($)	Total NPC ($)	Investment ($)	Saving ($)	SIR
0.00	0.40	76,460,577.95	76,460,577.95	0.00	0.00	—
0.50	0.80	74,331,372.40	76,163,951.01	1,832,578.61	2,129,205.55	1.16
0.50	1.20	73,331,635.79	75,537,873.40	2,206,237.61	3,128,942.16	1.42
0.50	1.60	72,345,887.00	74,925,783.60	2,579,896.61	4,114,690.95	1.59
0.50	2.00	71,374,706.87	74,328,262.48	2,953,555.61	5,085,871.08	1.72
1.00	0.80	72,878,232.54	76,169,730.75	3,291,498.21	3,582,345.41	1.09
1.00	1.20	71,871,269.39	75,536,426.60	3,665,157.21	4,589,308.56	1.25
1.00	1.60	70,877,737.50	74,916,553.71	4,038,816.21	5,582,840.46	1.38
1.00	2.00	69,789,591.64	74,202,066.85	4,412,475.21	6,670,986.31	1.51
2.00	0.80	69,333,955.39	75,543,292.81	6,209,337.42	7,126,622.56	1.15
2.00	1.20	68,349,676.42	74,932,672.84	6,582,996.42	8,110,901.53	1.23
2.00	1.60	67,270,851.59	74,227,507.01	6,956,655.42	9,189,726.36	1.32
2.00	2.00	66,199,028.78	73,529,343.20	7,330,314.42	10,261,549.17	1.40

annual growth scenario is considered for the electricity pool price. A 0% and a 1% annual growth scenario is considered for the electricity demand. This results in eight equally probable scenarios used across the 15-year planning horizon. The nominal rating sets for the BESS and PV in MW are determined as $\{0.5, 1, 2\}$ and $\{0.8, 1.2, 1.6, 2\}$, respectively. The BESS has a C-rate of 0.25.

D. Numerical Results and Analysis

Table IV, and Figures 7 and 8 present a summary of the operational net present cost (NPC), total NPC, investment costs, operation savings, and the saving-to-investment ratio (SIR) [27] for a range of PV and BESS configurations. Each scenario optimization encountered an insignificant number of infeasible days, 0.6% at most, attributed to solver memory issues. To account for these infeasible days, the operation cost of infeasible days was replaced by the average operation cost. The results demonstrate that as the PV capacity increases, regardless of the BESS size, operational NPC decreases due to the decreased reliance on electricity purchases from the grid and reduced generation from the CHP plant. Moreover, it is observed that the rate of increase in operational savings exceeds the incremental rate of PV investment, resulting in a strictly increasing SIR for PV installation.

Regarding the BESS, the results show a decreasing operational and total NPC as the BESS size increases. On the other hand, the SIR, signifying the returns per unit investment, follows the reverse trend; the maximum SIR of 1.72 is observed for a moderate BESS investment of 0.5 MW paired with 2.0 MW PV. Increasing BESS beyond 0.5 MW at the maximum PV capacity results in a reduced incremental economic benefit as SIR drops to 1.51 at 1 MW BESS and further to 1.40 at 2 MW BESS. Thus, the findings suggest diminishing returns with larger BESS installations, where the marginal increase in benefits reduces as the BESS capacity grows.

The findings motivate optimization with continuous variables for PV and BESS sizes, which is deferred to future work. Saying that, it is intuitive for the BESS-PV duo to have an inflection point in the SIR function. Comparing the NPC and SIR values across all scenarios reveals that the lowest NPC, equal to ∼$73.5M, belongs to the scenario with the highest

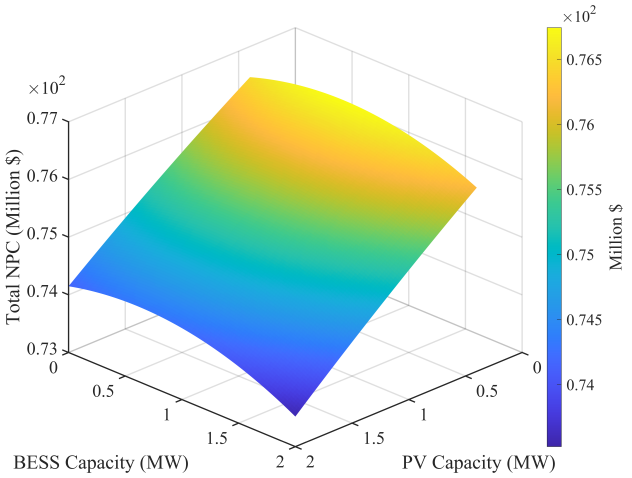

Fig. 7. Total NPC vs PV-BESS configurations

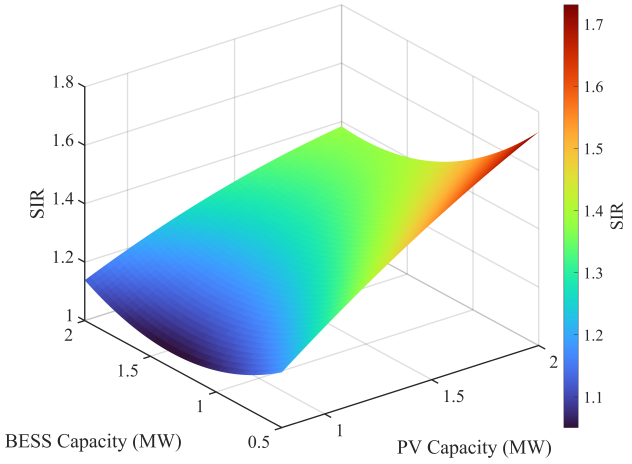

Fig. 8. SIR vs PV-BESS configurations

PV and BESS capacities, 2 MW each. On the other hand, the highest SIR, equal to 1.72, is achieved for a 0.5 MW BESS and 2.0 MW of PV. The analysis supports investing in increased PV capacities complemented by moderate-sized BESS to maximize economic returns, aligning with campus objectives of efficiency, reliability, and sustainability.

IV Conclusion and Future Works

This study presents stochastic planning for the University of Calgary campus microgrid over a 15-year planning horizon. The framework is based on practical data and considers the realistic constraints of the CHP plant and the intricacies of the campus electricity bill. The results support investment in PV paired with moderate-sized BESS, given the diminishing return per unit of investment as the BESS capacity increases. Note that higher BESS capacities still yield lower total NPC, and thus may be further justified by the campus resiliency mandates. Future works include:

- Carrying out sensitivity analysis to pool price profiles.
- Exploring the impact of operational energy forecasting accuracies on the planning study findings.
- Expanding studies to networked microgrids, considering continuous variables for the PV and BESS capacity.
- Determining the optimal distributed siting of PV and BESS units on campus, considering the networked microgrid operational and power flow constraints.
- Developing an EMS accounting for the networked microgrid structure, as well as operational constraints, including power flows and BESS degradation.
- Conducting transient and stability feasibility studies for grid-connected and islanded operation modes.

Acknowledgment

We extend our gratitude to the University of Calgary Energy and Utilities team, Mr. Earl Badger and Mr. Karl Steiner, who provided us with operational insight and data. This study was jointly funded by the University of Calgary VPR Catalyst Grant, including contributions from the University of Calgary Energy and Utilities Department, and Alberta Innovates Digital Innovation in Clean Energy (DICE) program.

Git Repository: https://github.com/DGRI-Lab/Campus-Microgrid-Stochastic-Planning.git

References

[1] Microgrid Knowledge, "Campus microgrids emerge as solution to energy challenges in higher education," Accessed: Mar. 15, 2024. [Online]. Available: https://www.microgridknowledge.com/resources/article/11428856/campus-microgrids-emerge-as-solution-to-energy-challenges-in-higher-education, 2020.

[2] D. Ton and M. Smith, "The U.S. Department of Energy's microgrid initiative," *Electricity J.*, vol. 25, no. 8, pp. 84–94, Oct. 2012.

[3] P. Sreedharan, J. Farbes, E. Cutter, C.-K. Woo, and J. Wang, "Microgrid and renewable generation integration: University of California, San Diego," *Appl. Energy*, vol. 169, pp. 709–720, 2016.

[4] H. Abd ul Muqeet, H. M. Munir, A. Ahmad, I. A. Sajjad, G.-J. Jiang, and H.-X. Chen, "Optimal operation of the campus microgrid considering the resource uncertainty and demand response schemes," *Math. Probl. Eng.*, vol. 2021, no. 1, p. Art. no. 5569701, 2021.

[5] A. B. Northmore and E. F. El-Saadany, "Analyzing the economic potential for DG CHP systems at the University of Guelph," in *Proc. 2012 IEEE Int. Conf. Power Energy (PECon)*, Dec. 2012, pp. 83–88.

[6] B. H. Vu, M. Husein, H.-K. Kang, and I.-Y. Chung, "Optimal design for a campus microgrid considering ESS discharging incentive and financial feasibility," *J. Elect. Eng. Technol.*, vol. 14, pp. 1095–1107, 2019.

[7] J. Lu, D. Lubkeman, N. Lu, T. Sun, and Z. Li, "An optimal microgrid dispatch algorithm for scheduling multiple CHPs in islanding operations," in *Proc. 2017 IEEE Power Energy Soc. Gen. Meeting (PESGM)*, 2017, pp. 1–5.

[8] B. Papari, C. S. Edrington, I. Bhattacharya, and G. Radman, "Effective energy management of hybrid AC–DC microgrids with storage devices," *IEEE Trans. Smart Grid*, vol. 10, no. 1, pp. 193–203, 2017.

[9] X. Wang, S. Chen, Y. Zhou, J. Wang, and Y. Cui, "Optimal dispatch of microgrid with combined heat and power system considering environmental cost," *Energies*, vol. 11, no. 10, p. Art. no. 2493, 2018.

[10] B. V. Solanki, K. Bhattacharya, and C. A. Canizares, "A sustainable energy management system for isolated microgrids," *IEEE Trans. Sustain. Energy*, vol. 8, no. 4, pp. 1507–1517, 2017.

[11] H. Kanchev, D. Lu, F. Colas, V. Lazarov, and B. Francois, "Energy management and operational planning of a microgrid with a PV-based active generator for smart grid applications," *IEEE Trans. Ind. Electron.*, vol. 58, no. 10, pp. 4583–4592, 2011.

[12] X. Ge and J. Khazaei, "Physics-informed convolutional neural network for microgrid economic dispatch," *Sustain. Energy, Grids Netw.*, vol. 40, p. Art. no. 101525, 2024.

[13] H. Jiang, S. Ning, and Q. Ge, "Multi-objective optimal dispatching of microgrid with large-scale electric vehicles," *IEEE Access*, vol. 7, pp. 145 880–145 888, 2019.

[14] G. Li, R. Zhang, T. Jiang, H. Chen, L. Bai, H. Cui, and X. Li, "Optimal dispatch strategy for integrated energy systems with CCHP and wind power," *Appl. Energy*, vol. 192, pp. 408–419, 2017.

[15] W. Violante, C. A. Cañizares, M. A. Trovato, and G. Forte, "An energy management system for isolated microgrids with thermal energy resources," *IEEE Trans. Smart Grid*, vol. 11, no. 4, pp. 2880–2891, 2020.

[16] L. Guo, W. Liu, J. Cai, B. Hong, and C. Wang, "A two-stage optimal planning and design method for combined cooling, heat and power microgrid system," *Energy Convers. Manage.*, vol. 74, pp. 433–445, 2013.

[17] Y. Xu and Z. Deng, "Bi-level planning of microgrid considering seasonal hydrogen storage and efficiency degradation of electrolyzer," *IEEE Trans. Ind. Appl.*, vol. 61, no. 1, pp. 1385–1398, 2025.

[18] M. Amini, M. B. Sanjareh, M. H. Nazari, G. B. Gharehpetian, and S. H. Hosseinian, "A novel model for battery optimal sizing in microgrid planning considering battery capacity degradation process and thermal impact," *IEEE Trans. Sustain. Energy*, vol. 15, no. 3, pp. 1435–1449, 2024.

[19] J.-M. Ling and F. I. Mulani, "Planning and optimization of a residential microgrid utilizing renewable resources and integrated energy storage," *J. Energy Storage*, vol. 97, p. Art. no. 112933, 2024.

[20] Alberta Electric System Operator, "(AESO)," Accessed: Sep. 15, 2024. [Online]. Available: https://www.aeso.ca/, 2023.

[21] City of Calgary, "Energy costs: Understanding your city energy bill," Accessed: Feb. 15, 2025. [Online]. Available: https://www.calgary.ca/our-finances/facts/energy-costs.html?redirect=/franchisefees, 2024.

[22] E. G. Vera, C. A. Cañizares, M. Pirnia, T. P. Guedes, and J. D. M. Trujillo, "Two-stage stochastic optimization model for multi-microgrid planning," *IEEE Trans. Smart Grid*, vol. 14, no. 3, pp. 1723–1735, 2023.

[23] National Renewable Energy Laboratory, "2024 annual technology baseline: Commercial battery storage," Accessed: Feb. 15, 2025. [Online]. Available: https://atb.nrel.gov/electricity/2024/commercial_battery_storage, 2024.

[24] Caterpillar Inc., "Solar turbine titan 130 gas turbine generator set," Accessed: Feb. 15, 2025. [Online]. Available: https://s7d2.scene7.com/is/content/Caterpillar/CM20150703-52095-43744, 2015.

[25] ENMAX, "2025 interim rate schedule," Accessed: Feb. 15, 2025. [Online]. Available: https://media.auc.ab.ca/prd-wp-uploads/Shared%20Documents/Rates/Appendix%203-ENMAX-2025-interim-rate-schedule.pdf, 2025.

[26] Alberta Energy Regulator, "Aeco-c natural gas price," Accessed: Feb. 15, 2025. [Online]. Available: https://www.aer.ca/data-and-performance-reports/statistical-reports/alberta-energy-outlook-st98/prices-and-capital-expenditure/natural-gas-prices/aeco-c-price, 2024.

[27] National Institute of Standards and Technology, "Nist handbook 135: Life-cycle costing manual for the federal energy management program," Accessed: Feb. 15, 2025. [Online]. Available: https://nvlpubs.nist.gov/nistpubs/hb/2020/NIST.HB.135-2020.pdf, 2020.